Journal of Marine Science and Technology

Volume 25 | Issue 6 Article 8

INVESTIGATION OF EFFECTS OF WAVE DIRECTIONS ON HULL WAVE LOADS BY HYDROELASTIC EXPERIMENTAL METHOD

Zhanyang Chen
College of Naval Architecture and Ocean Engineering, Harbin Institute of Technology at Weihai, Weihai, Shandong, China., chen_1228@163.com

Jialong Jiao
School of Civil Engineering and Transportation, South China University of Technology, Guangzhou, China.

Recommended Citation

Chen, Zhanyang and Jiao, Jialong (2017) "INVESTIGATION OF EFFECTS OF WAVE DIRECTIONS ON HULL WAVE LOADS BY HYDROELASTIC EXPERIMENTAL METHOD," *Journal of Marine Science and Technology*: Vol. 25: Iss. 6, Article 8.
DOI: 10.6119/JMST-017-1226-08
Available at: https://jmstt.ntou.edu.tw/journal/vol25/iss6/8

INVESTIGATION OF EFFECTS OF WAVE DIRECTIONS ON HULL WAVE LOADS BY HYDROELASTIC EXPERIMENTAL METHOD

Acknowledgements

This work was supported by National Natural Science Foundation of China (Grant No. 51509062), State Key Laboratory of Ocean Engineering (Shanghai Jiao Tong University) (Grant No. 1416), Science and technology development projects of Weihai (2015DXGJMS009), and the Fundamental Research Funds for the Central Universities (Grant No. HIT.NSRIF.201727).

Journal of Marine Science and Technology, Vol. 25, No. 6, pp. 680-688 (2017)
DOI: 10.6119/JMST-017-1226-08

INVESTIGATION OF EFFECTS OF WAVE DIRECTIONS ON HULL WAVE LOADS BY HYDROELASTIC EXPERIMENTAL METHOD

Zhanyang Chen[1] and Jialong Jiao[2]

Key words: hydroelasticity, ship model experiment, wave direction, load responses.

ABSTRACT

This paper focuses on the hydroelastic responses of ultra-large vessels under different wave directions. Segmented ship model experiments provide an invaluable tool in naval applications. However, most model tests are performed on heading waves. Therefore, a segmented model with variable cross-section steel backbones was designed and the oblique wave tests were performed in a comprehensive test tank. The oblique wave test system was introduced in detail. Time histories of bending moments in oblique waves were given. In order to analyze the influence of structural elastic effect on hydroelastic responses, the number of segments of the model was changed, and the variation of the high frequency slamming bending moments and low frequency wave bending moments with wave directions was analyzed. It is shown that compared with the low frequency wave moments, the high frequency load responses are more sensitive to the change of wave direction. Finally, numerical simulations of the ship load responses were carried out by using three-dimensional nonlinear hydroelastic method. The computational results under different wave directions have been correlated with those from model tests.

I. INTRODUCTION

With increasing demands for huge dimensions and high-speed transportation, ship designers are confronted with the challenge of reducing the weight through the use of light-weight materials. This makes the structure more flexible and hull natural frequency lower, which leads to whipping easily. For ultra-large vessels, in order to predict wave loads accurately, segmented model experiment is one of the important methods that verify elastic effect of the hull on the wave loads (Lewis, 1954). In recent decades, great progress has been made in segmented model experiment investigation. Jiao et al. (2015) improved the traditional towing test method used by Wang et al. (2012) and presented a segmented self-propelling model to study hull girder vibrations and wave impact response of a large ship in regular waves. Chen and Ren (2013) utilized variable cross-section backbone system to simulate the stiffness distribution of hull respectively. Compared to uniform backbone system (Rousset et al., 2010), the variable cross-section backbone can better reproduce mechanical properties of hull. Moreover, Jiao et al. (2015 and 2016) proposed the large-scale model tests in actual sea state to replace the tests in towing tank (Drummen et al., 2009; Panciroli et al., 2009). They concluded that large-scale model tests carried out at sea were more reliable for ship design and scientific research. Though the test method is becoming more and more mature, due to the limitations of current test technique and test site, published papers are limited to experimental data in heading waves.

In addition, whipping responses can be studied by hydroelastic theory (Oberhagemann and Moctar, 2012; Kim et al., 2013; Drummen and Holtmann, 2014). However, slamming is the strongly nonlinear phenomenon which related to various factors, such as bow linetype, ship-wave vertical relative speed. It is difficult to obtain the exact solution through the numerical simulation. Especially the changes of whipping responses with the wave direction have drawn relevant scholars' attentions in recent years. Model test provides a general method to allow for full nonlinearity of waves.

Firstly, for the hydroelastic tests in oblique waves, a segmented ship model of a 13000-TEU container ship was adopted in this paper. The designs of the ship model and the oblique wave testing system were introduced in detail. Secondly, experimental procedures and results were described, including the model's response data under different wave directions. Finally, based on three-dimensional (3D) nonlinear hydroelastic theory, numerical simulations of the hydroelastic responses of the ship in oblique regular waves were also carried out. The analysis of the numerical results by the presented method shows good agreement with experimental results.

Paper submitted 06/14/17; revised 08/22/17; accepted 10/30/17. *Author for correspondence: Zhanyang Chen (email: chen_1228@163.com).*
[1] *College of Naval Architecture and Ocean Engineering, Harbin Institute of Technology at Weihai, Weihai, Shandong, China.*
[2] *School of Civil Engineering and Transportation, South China University of Technology, Guangzhou, China.*

Table 1. Main parameters of the model.

Principal dimension	Prototype ship	Model
Length overall/m	349.5	4.66
Length waterline /m	331.5	4.42
Breadth /m	43.5	0.58
Depth /m	31.5	0.42
Draft /m	14.25	0.19
Displacement /t	104625	0.248

Fig. 1. The comprehensive test tank of HEU.

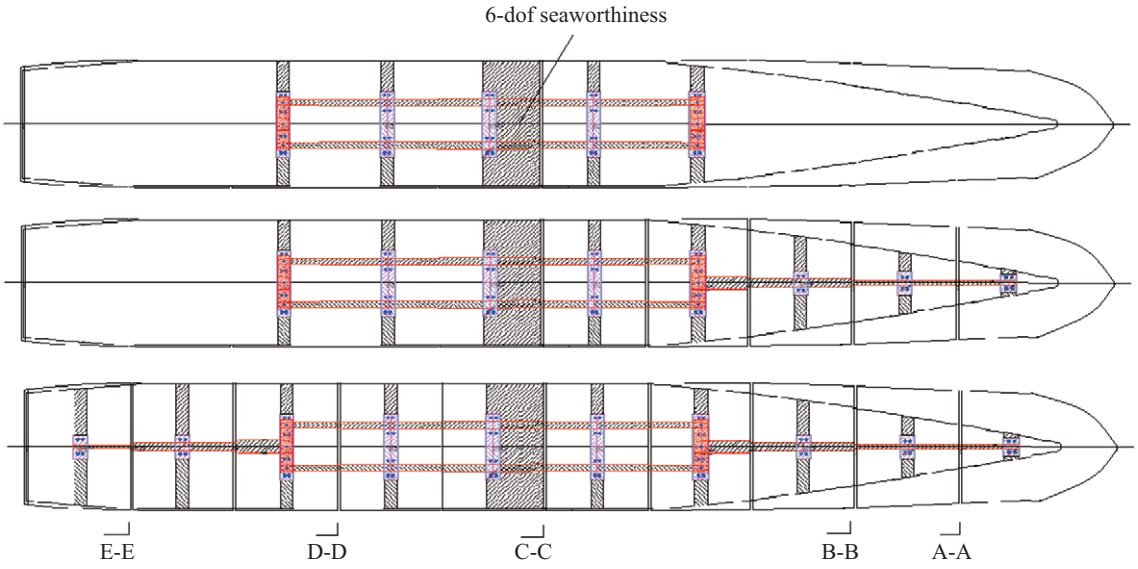

Fig. 2. Ship model with different segments.

II. HYDROELASTIC EXPERIMENT METHOD

1. Model Setup

The hydroelastic experiment in this paper was carried out in the comprehensive test tank of Harbin Engineering University (HEU). Principal dimensions for the tank are 50 m × 30 m × 10 m. The trailer system in the tank can be 360-degree rotated, so tests in arbitrary heading waves (β= 0°-360°) can be carried out. Fig. 1 is the comprehensive test tank of HEU. In order to investigate the wave load characteristics, a segmented ship model that was made of fiberglass reinforced plastic was built. The scale ratio of the model was chosen as 1:75 as a compromise between the model manufacture and testing requirements. The main parameters of the model are shown in Table 1. The model was cut into two parts, six parts and ten parts of segmented hulls respectively. The gaps between each two segmented hulls were 1 cm. There was a steel backbone system fixed at the vertical bending neutral axis of the model. Unlike the traditional segmented model that is constructed with uniform beams, in order to make the stiffness and weight distribution of model consis-

Table 2. Comparison between theoretical and experimental natural frequency of the model.

Natural frequency	Calculation results (Hz)	Test results (Hz)					
		2-segment model	Error 1	6-segment model	Error 2	10-segment model	Error 3
First order	6.31	9.03	43.11%	7.45	18.07%	6.41	1.58%
Second order	15.18	——	——	18.1	19.24%	14.02	7.64%
Third order	26.59	——	——	——	——	24.4	8.24%

(a) The first order displacement mode (b) The second order displacement mode (c) The third order displacement mode

Fig. 3. The natural vibration mode along ship based on FEM.

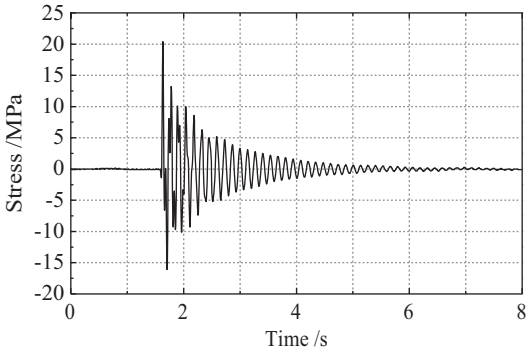

Fig. 4. Time traces of stress of 10-segment model.

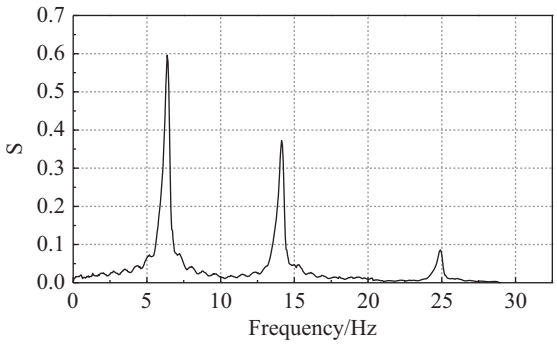

Fig.5. Natural frequency of 10-segment model.

tent with the prototype ship, the variable cross-section beams were used to simulate the stiffness of the hull. Arrangements of the model and the measuring equipment installed on the model are schematized in Fig. 2. Fig. 3 shows the vertical displacement mode shapes along the ship length of first three orders of the prototype ship calculated by finite element method (FEM). Before the wave load tests, the impact hammer tests in calm water were performed firstly, which can verify whether the design of backbones satisfies the requirements of the experiment. The time traces of stress amidships were obtained and shown in Fig. 4. Spectral analysis based on the Fourier Transform Method (FFT) was performed to identify the natural frequency of ship model, as shown in Fig.5.

The measured and simulated wet natural frequencies are summarized in Table 2. As shown in Table 2, a good agreement between the prediction and 10-segment model experiment is found for the first order vertical bending mode. The results measured are larger than the calculated. Moreover, the error between tested and calculated frequencies increases with the increasing order of mode, i.e., from the first order natural frequency to the third order natural frequency. The errors in terms of the 10-segment model are 1.58% and 8.24% corresponding to the first order and the third order natural frequencies, respectively. However, the tested two-node natural frequency of the 2-segment model shows pronounced departure from the expected, with an error of 43.11%. In addition, as seen from the frequency domain result of the 2-segment model, the high order vibrational frequencies are hard to be identified since the corresponding energy components are not pronounced. This indicates that the advantages of using model with more segments are obvious.

2. Oblique Wave Testing System

The model tests were performed in long-crested regular waves. Wave direction angles of 0° (heading wave), 30°, 45°, 60°, 90° (beam sea), 120° and 150° were selected. Rule of the wave direction angle is shown in Fig. 6.

The testing system utilized mainly comprises towing facility and the testing model, which is shown in Fig. 7. Signals, including motions and sectional loads, were collected by means of a

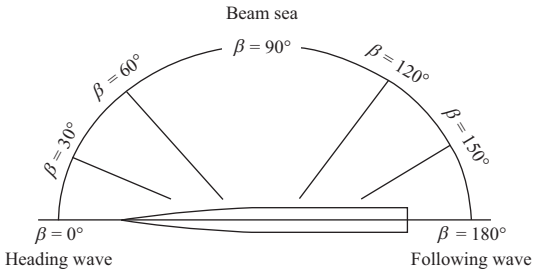

Fig. 6. Rule of the wave direction angle.

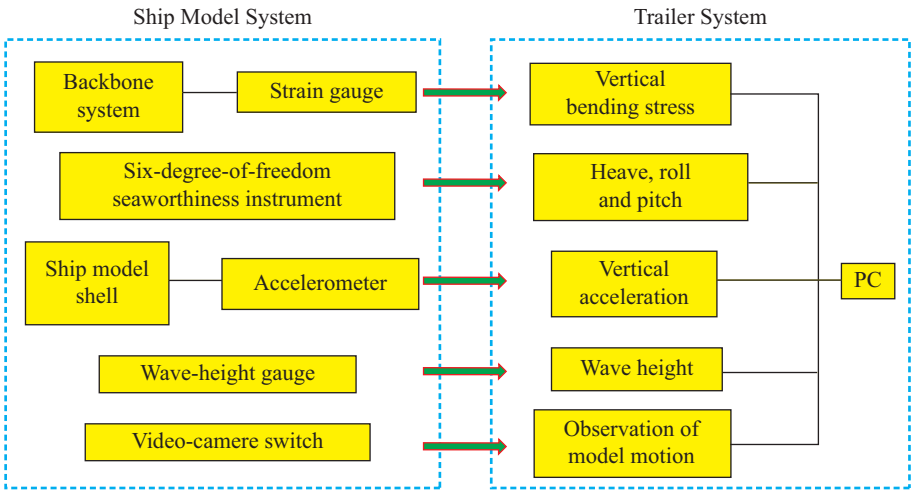

Fig. 7. Flowchart of the test control system.

Fig. 8. Six-degree-of-freedom seaworthiness instrument.

Fig. 9. The ship model launching.

data collector onboard the towing carriage. Moreover, the signals of motions and loads were transferred to the data collector through a local cable. The computations were made on an 8 CPU workstation with 3.4 GHz, on windows Win 7 system.

Test contents and instruments used are as follows:

(1) Waves were made by a hydraulically driven wave maker of the multiple flap type, which generated regular and irregular waves. The largest wave height of regular wave was 0.4 m, The largest significant wave heights of irregular wave was 0.3 m. The wave period was within 0.5 s - 4.0 s;
(2) Vertical bending moment (VBM) at the sections A-E were measured by strain gauges, which were glued onto the surface of the backbone, using a full-bridge circuit. The sampling frequency was set at 200 Hz during the tests;
(3) The model movements were measured by six-degree-of-freedom seaworthiness instrument. The seaworthiness instrument is shown in Fig. 8;
(4) Wave-height gauge was used to measure wave height;
(5) Accelerometers were located on the model shell to measure the vertical acceleration;
(6) Two video cameras were mounted on the carriage in order to record the sailing state of the model.

Fig. 9 shows the ship model launching.

Table 3. Proportions of HF and LF bending moments of different segmented models.

Model	Condition 1 (v = 24 kn, h = 7 m, λ/L = 1.0)		Condition 2 (v = 8 kn, h = 17.5 m, λ/L = 1.0)	
	M_{HF}	M_{LF}	M_{HF}	M_{LF}
2-segment model	9.55%	90.45%	30.58%	69.42%
6-segment model	26.90%	73.10%	48.31%	51.69%
10-segment model	33.12%	66.88%	79.55%	20.45%

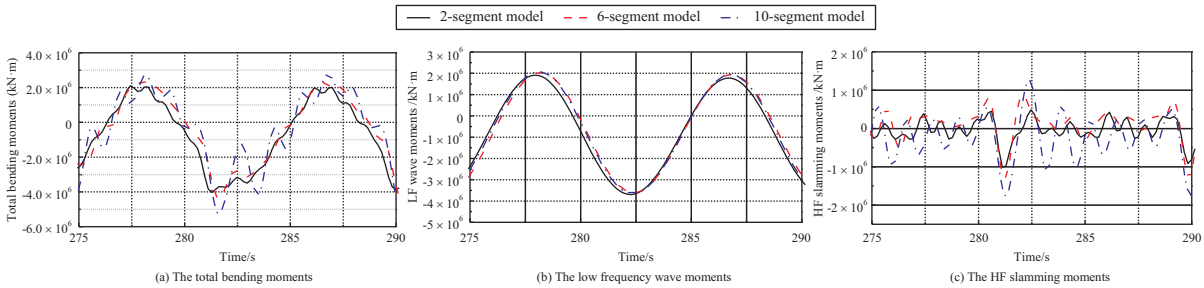

Fig. 10. Time histories of VBM of different segmented models.

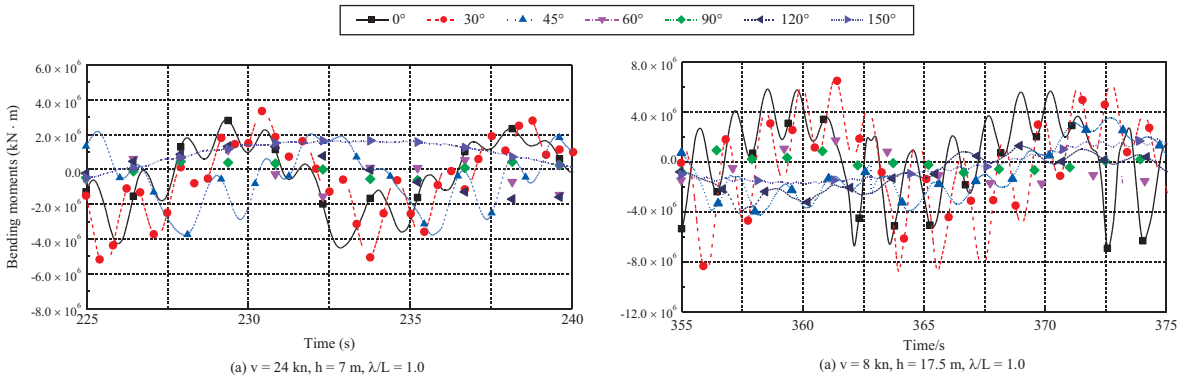

Fig. 11. Time histories of VBM under different wave directions.

III. TESTING RESULTS AND ANALYSES

1. The Time History of Test Data

The time histories of VBM amidships of three different segmented models for corresponding sea state (sailing speed v = 24 kn, wave height h = 7 m, ratio of wave length to ship length λ/L = 1.0) are reported in Fig. 10. It is known that the loads experienced by ships in severe waves can be split into two categories: The low frequency (LF) wave loads and high frequency (HF) slamming loads. Usually these two kinds of load oscillate at different frequencies. In this paper the LF bending moments caused by waves and HF bending moments caused by bow impact were separated by Fourier filter. It is observed from Fig. 10 that the LF wave bending moments measured did not change obviously, and only slight HF load responses have taken place in 2-segment model test results. With increasing number of segment, the HF load responses increase rapidly. There is obvious whipping component in 10-segment model test.

It should be noticed that the results in Fig. 10 are measured in the same condition, the whipping occurs only in the 10-segment model test. Comparisons of slamming pressures among different segmented models were performed. It is found that the number of model segment has little influence on slamming pressure, and these three models encounter the same slamming pressure. This means that change of elastic effect of ship leads to the different results. It can be concluded that the smaller natural frequency the ship is, the higher whipping responses are. In order to emphasize the ratios of HF and LF bending moments to the total bending moments of different segmented models, the ratios of HF slamming moments and LF wave moments in two typical conditions are shown in Table 3. As seen from the results, the HF load responses of 10-segment model test are larger than those of other tests, With the increasing of wave height, this feature becomes more obvious. In analysis of the high sea state, model with fewer segments may introduce error.

Therefore, in order to study hydroelastic responses clearly, the 10-segment model experimental results will be discussed in the following. Fig. 11 shows time histories of VBM amidships

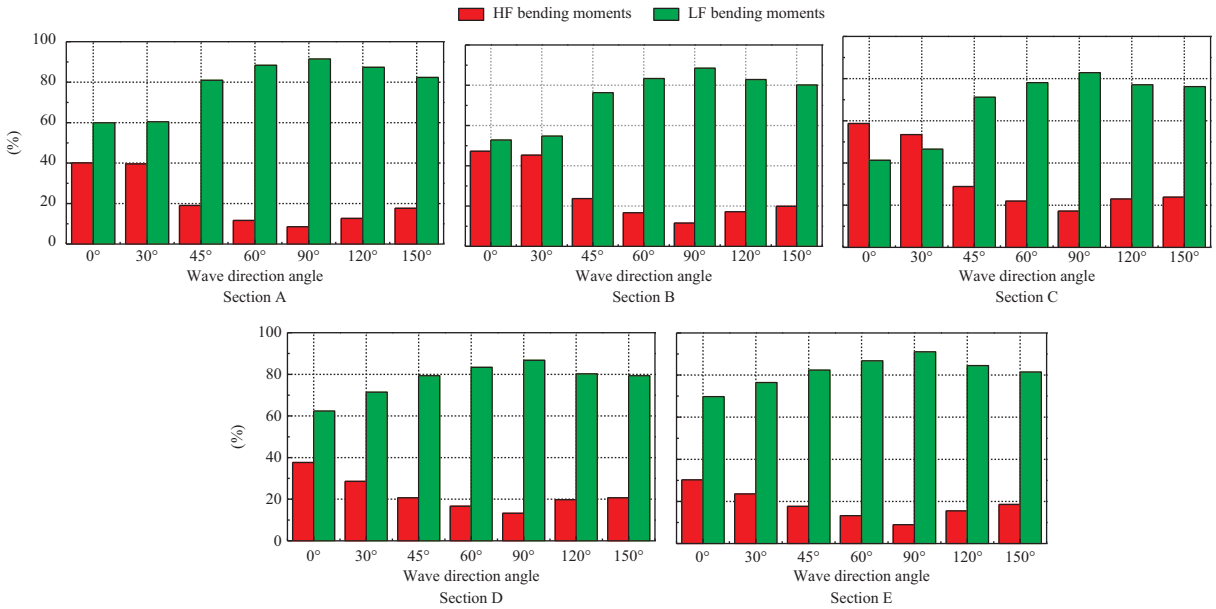

Fig. 12. Ratios of components load to combined VBM load under different wave direction (v = 8 kn, h = 17.5 m, λ/L = 1.0).

under different wave directions in these two typical conditions. As seen from the results, the time series of VBM amidships corresponding to different wave direction angles show periodicity. The model in bow seas experiences more waves than that in quartering sea in the same time interval.

The results in the figures show the largest total bending moments occur in the heading angle of β = 30°, and HF vibration characteristic in the heading wave is most significant. With increasing wave direction angle, HF vibration characteristic would decay. In the same condition, wave direction has a more effect on HF load responses, this is because wave encounter frequency of following waves is smaller than that of heading waves. From the formula (1), with increasing wave direction angle, the wave encounter frequency is smaller and smaller, the difference between natural frequency (f_{1st} = 6.41 Hz → f_{2nd} = 16.02 Hz → f_{3rd} = 29.40 Hz) and encounter frequency is getting greater. It is shown that the main influencing factor on the HF vibration responses is the difference between natural frequency and encounter frequency for a given ship speed and wave height.

$$\omega_e = 2\pi\frac{v\cos\beta + c}{\lambda} = 2\pi\frac{v\cos\beta + \sqrt{\frac{g\lambda}{2\pi}}}{\lambda} = \omega + \frac{\omega^2 v\cos\beta}{g} \quad (1)$$

In addition, the HF load responses in heading and bow waves significantly increase with increasing sea states comparing with those in quartering sea, and the HF load responses in beam seas are almost unchanged.

2. Variation of Test Data

Since the measured bending moments are comprised of LF wave bending moments and HF slamming bending moments, the ratios of LF bending moments and HF bending moments to total bending moments at section A-E were calculated and shown in Fig. 12.

From the comparison, it can be concluded that the largest ratio of HF bending moments occurs at section C, which is the amidships division. For the VBM, when the wave direction angle is close to 90°, there are decreases in the ratio of HF bending moments to total bending moments. In the same condition, the ratio of HF bending moments to total bending moments in heading wave is 58.73%, the ratio in beam wave is 17.17%. The same trend can be found at other sections. When wave direction angle is greater than 90°, there are significant increases in the ratio of HF bending moments to total bending moments with increasing wave direction angle. It is necessary to pay enough attention to the effects of wave direction angle on load responses. The VBM amidships corresponding to different wave direction angles and ratio of wave length to ship length were calculated. The dimensionless results are shown in Fig. 13.

The dimensionless method of VBM is as follows:

$$M_{\text{dimensionless}} = \frac{M}{\rho g \zeta_a L^2 B} \quad (2)$$

where, ρ is the density of water; g is acceleration of gravity; ζ_a is the wave amplitude; L is ship waterline length; B is ship breadth.

As seen from the results, for the different ratios of wave length to ship length, the variation of VBM amidships with wave direction angle is very identical. When β = 0-90°, there are decreases in the measuring data with increasing wave direction angle; when β = 90°-150°, there are significant increases in the measuring data with increasing wave direction angle; when β = 90°, the results are minimum; when β = 30°, the results are maximum. For the different wave direction angles, however, the

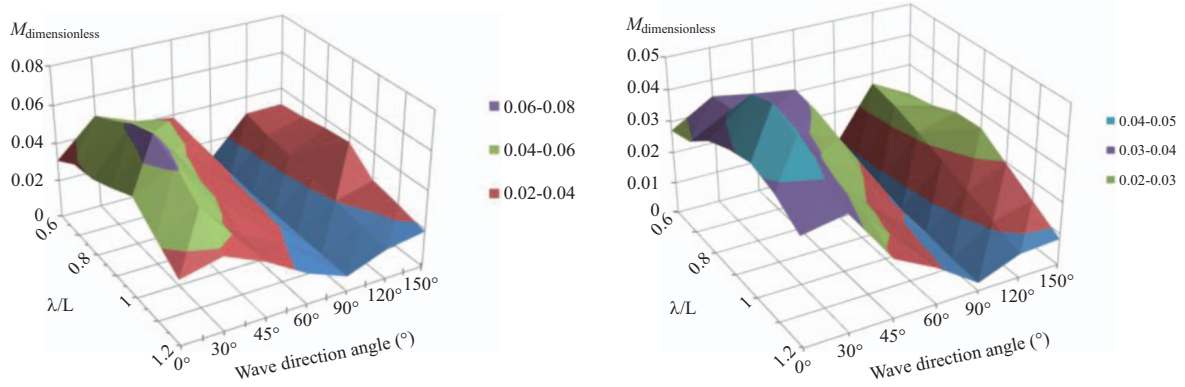

(a) v = 20 kn, h=7 m (b) v = 8 kn, h = 17.5 m

Fig. 13. Dimensionless results of VBM amidships.

change trendence of VBM with λ/L is different. When β= 0-90°, the maximum value of VBM occurs near λ/L = 1.0; when β = 30° and 150°, the maximum values occur near λ/L = 0.9; when β = 45°, the maximum value occurs near λ/L = 0.7; when β = 60° and 120°, the maximum values occur near to λ/L = 0.6. It can be concluded that the maximum values of VBM occur at $\lambda/(L\cdot\cos\beta)$ = 1.0 in oblique waves, which is different from that in heading wave.

IV. NUMERICAL SIMULATION

1. Nonlinear Hydroelastic Method

In this paper, a 3-D nonlinear hydroelastic method is presented to predict wave loads of the container ship at different wave directions (Chen et al., 2015). The two nonlinear factors are considered: instantaneous-body nonlinearity and slamming forces. The hydroelastic motion equation is expressed as

$$\begin{aligned}&([a]+[A])\ddot{p}_r(t)+([b]+[B])\dot{p}_r(t)+([c]+[C])p_r(t)\\&=\{F_I(t)\}+\{F_D(t)\}+\{F_{slam}(t)\}\end{aligned} \tag{3}$$

where, [A], [B], and [C] are generalized fluid added mass, damping coefficient, and stiffness matrices, respectively; [a], [b], and [c] are generalized structural mass, damping coefficient, and stiffness matrices, respectively; P_r(t) is the r-th mode principal coordinates; $F_I(t)$ is incident wave force; $F_D(t)$ is dispersion wave force; $F_{slam}(t)$ is slamming force.

Since the position of the ship relative to the wave changes all the time, the fluid forces were calculated on the instantaneous wetted surface of the hull by the time domain method. For the calculation of the wave exciting force in regular waves, with the help of the interception of instantaneous grid, the incident wave force and diffraction wave force on the instantaneous wetted body surface can be given as:

$$\begin{cases}F_I(t)=-\rho\zeta_a\iint\limits_{S(t)}\vec{n}\cdot\vec{u}_r(i\omega-U\dfrac{\partial}{\partial x})\phi_0 ds\\ F_D(t)=-\rho\zeta_a\iint\limits_{S(t)}\vec{n}\cdot\vec{u}_r(i\omega-U\dfrac{\partial}{\partial x})\phi_d ds\end{cases}(r=1,2,\ldots m) \tag{4}$$

where, ϕ_0 and ϕ_d are instantaneous incident potential and diffraction potential per wave amplitude respectively; $\vec{n}$ is the normal vector, which is defined positive when pointing into body from the boundary surface; $\vec{u}_r$ is the r-th principal modes of the structure.

Radiation force on the instantaneous wetted body surface is written as

$$\{F_R(t)\}=-[A_{rk}(t)]\{\ddot{p}_r(t)\}-[B_{rk}(t)]\{\dot{p}_r(t)\} \tag{5}$$

where, $A_{rk}(t)$ is added mass; $B_{rk}(t)$ is damping coefficient.

$$\begin{cases}A_{rk}=\dfrac{-\rho}{\omega^2}\mathrm{Re}\iint\limits_{S(t)}\vec{n}\cdot\vec{u}_r(i\omega-U\dfrac{\partial}{\partial x})\phi_k ds\\ B_{rk}=\dfrac{\rho}{\omega}\mathrm{Im}\iint\limits_{S(t)}\vec{n}\cdot\vec{u}_r(i\omega-U\dfrac{\partial}{\partial x})\phi_k ds\end{cases}(r,k=1,2,\ldots,m)$$

Slamming caused by large amplitude motion of hull was also taken into account in the study. In this paper, momentum impact theory is adopted to calculate the bow flare impact force:

$$F_{slam}(x,t)=-\{\frac{d}{dt}[m(x,t)\frac{d}{dt}Z_R(x,t)]-\rho g s(x,t)\} \tag{6}$$

where, $m(x, t)$ is the instantaneous added mass; $Z_R(x, t)$ is vertical relative ship displacement to wave; $s(x, t)$ is instantaneous sinking area.

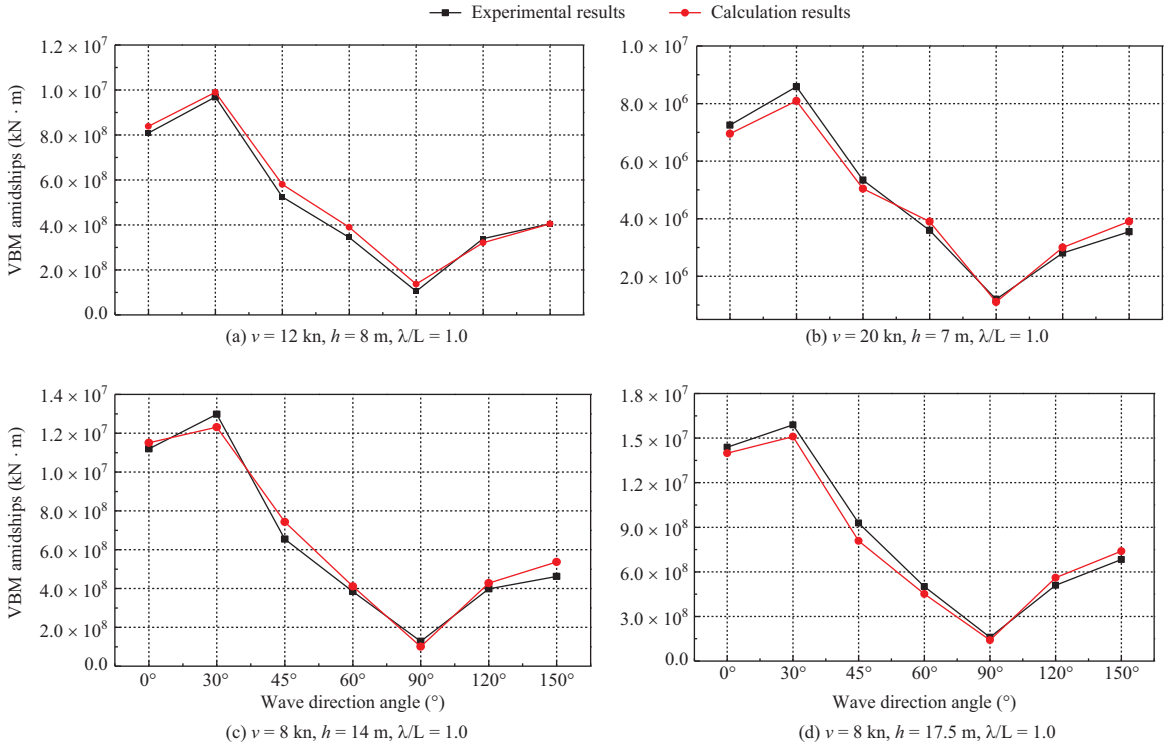

Fig. 14. Comparison of the results.

For the solution of the second-order differential motion Eq. (3), the fourth-order Runge-Kutta method has been adopted in this paper.

$$\begin{cases} y_{n+1} = y_n + \dfrac{1}{6}(K_1 + 2K_2 + 2K_3 + K_4) \\ K_1 = hf(x_n, y_n) \\ K_2 = hf(x_n + \frac{1}{2}h, y_n + \frac{1}{2}K_1) \\ K_3 = hf(x_n + \frac{1}{2}h, y_n + \frac{1}{2}K_2) \\ K_4 = hf(x_n + h, y_n + K_3) \end{cases} \tag{7}$$

Then based on modal superposition principle, the displacement, moment, and shearing force of a given cross section could be obtained:

$$\begin{cases} w(x,t) = \sum_{r=1}^{m} p_r(t) w_r(x) \\ M(x,t) = \sum_{r=1}^{m} p_r(t) M_r(x) \\ V(x,t) = \sum_{r=1}^{m} p_r(t) V_r(x) \end{cases} \tag{8}$$

where, $w_r(x)$, $M_r(x)$, and $V_r(x)$ are the r-th natural mode of displacement, moment, and shearing force, respectively. r = 1-6 denotes the rigid body motion modes of six degrees of freedom, while r = 7-m denotes the elastic hull deformation modes.

2. Comparison of the Results

Four conditions were selected for the comparison of peak-to-peak value of the total bending moments. The calculation results as well as the experimental results under different wave directions are shown in Fig. 14.

It is shown in Fig. 14 that the calculation results show good agreement with the experimental ones. The variation trends of the calculation data and experimental data are consistent. With increasing wave height, there are significant increases in both calculation and experimental results.

In the test conditions of β = 30°, the VBM amidships are 9687.198 MN · m and 8589.874 MN · m corresponding to wave heights of 8 m and 7 m, respectively (see Fig. 14(a) and 14(b)). However, the bending moments increased from 9687.198 MN · m to 15894.055 MN · m when the wave heights increased from 8 m to 17.5 m (see Fig. 14(a) and 14(d)). It is observed that the load responses increase rapidly, due to the serious slamming force, with higher wave height. However, the load responses in beam seas have no significant change in different conditions.

V. CONCLUSIONS

In this paper, a segmented ship model of a 13000-TEU container ship with steel variable cross-section backbone system was designed and the tests in oblique regular waves were per-

formed in a towing tank. Studies of hydroelastic responses have been conducted with comparative verification between numerical and experimental results in order to estimate the effect of wave directions on load responses. The following conclusions can be made:

(1) The first order natural frequency of the hull is used as a basis for designing the segmented model. For the model with fewer segments, the high order natural frequency cannot be measured, and the error caused by fewer segments is not ignorable, especially for load response analysis. Models with more segments have been suggested in this paper;
(2) Hull elastic effect has great influence on whipping responses, the smaller natural frequency the ship is, the higher whipping responses are, and vice versa;
(3) The maximum value of load responses occurs at $\beta = 30°$, however the most serious whipping is in heading wave, and the maximum bending moment in oblique waves is around $\lambda/(L \cdot \cos \beta) = 1.0$. Compared with the LF wave bending moments, the HF slamming bending moments are more sensitive to wave direction;
(4) From comparison with the segmented model experimental results in oblique waves, the 3-D nonlinear hydroelastic theory can consider the hull elastic effect accurately, and reflect the influence of wave direction on the load responses.

ACKNOWLEDGEMENTS

This work was supported by National Natural Science Foundation of China (Grant No. 51509062), State Key Laboratory of Ocean Engineering (Shanghai Jiao Tong University) (Grant No. 1416), Science and technology development projects of Weihai (2015DXGJMS009), and the Fundamental Research Funds for the Central Universities (Grant No. HIT.NSRIF.201727).

REFERENCES

Chen, Z. Y. and H. L. Ren (2013). Research on the design loads of a surface warship. Materials, Mechanical Engineering and Manufacture 268, 1-6.

Chen, Z. Y., G. C. Lu and G. H. He (2015). Hydroelastic analysis of effect of various nonlinear factors on load responses. The 25th The International Society of Offshore and Polar Engineers. Kona, USA, 759-763.

Drummen, I., M. K. Wu and T. Moanl (2009). Experimental and numerical study of containership responses in severe head seas. Marine Structures 22, 172-193.

Drummen, I. and M. Holtmann (2014). Benchmark study of slamming and whipping. Ocean Engineering 86, 3-10.

Jiao, J. L., H. L. Ren and C. A. Adenya (2015). Experimental and Numerical Analysis of Hull Girder Vibrations and Bow Impact of a Large Ship Sailing in Waves. Shock and Vibration, 1-10.

Jiao, J. L., H. L. Ren S. Z. Sun and C. A. Adenya (2015). Investigation of a ship's hydroelasticity and seakeeping performance by means of large-scale segmented self-propelling model sea trial. Journal of Zhejiang University-SCIENCE A (Applied Physics & Engineering) 16(5), 387-404.

Jiao, J. L, H. L. Ren, S. Z. Sun and C. A. Adenya (2016). Experimental Investigation of Wave-Induced Ship Hydroelastic Vibrations by Large-Scale Model Measurement in Coastal Waves. Shock and Vibration, 1-14.

Kim, Y., J. H. Kim and Y. Kim (2013). Whipping identification of a flexible ship using wavelet cross-correlation. Ocean Engineering 74, 90-100.

Lewis, E. V. (1954). Ship Model Tests to Determine Bending Moments in Waves. SNAME Transactions 9, 1-43.

Oberhagemann, J. and O. Moctar (2012). Numerical and experimental investigations of whipping and springing of ship structures. Offshore and Polar Engineering 22(2), 108-114.

Panciroli, R., S. Abrate, G. Minak and A. Zucchelli (2012). Hydroelasticity in water-entry problems: Comparison between experimental and SPH results. Composite Structures 94(2), 532-539.

Rousset, J., P. Ferrant and B. Alessandrini (2010). Experiments on a segmented ship model in directional irregular waves. Proceeding of International Workshop on Water Waves and Floating Bodies, Harbin, China.

Wang X. L., X. K. Gu, J. J. Hu and C. Xu (2012). Experimental Investigation of Springing Responses of a Large LNG Carrier. Shipbuilding of China 53(4), 1-12.